Vacuum-infrared Drying of Okra Slices: Kinetics, Quality Analysis, and Optimisation

F. SalehNezhad[1], Y. Mansoori[1*], S. M. Safieddin Ardebili[1]

1- Department of Biosystems Engineering, Shahid Chamran University of Ahvaz, Ahvaz, Iran
(*- Corresponding Author Email: y.mansoori@scu.ac.ir)
https://doi.org/10.22067/jam.2025.96137.1442

Abstract

Okra (*Abelmoschus esculentus* L.) slices were dried using vacuum-infrared drying method. A laboratory-scale dryer was designed and fabricated to control the drying parameters and monitor the weight change of samples. The parameters examined included temperature (50, 55, 65, 75, and 80ºC) and absolute pressure (5, 21, 53, 85, and 101 kPa). The response factors were drying time, drying rate, effective diffusivity, specific energy consumption, colour change (ΔE and a/a_0), and rehydration ratio. The results from the response surface methodology indicated that the optimal conditions for minimising drying time and maximising green colour preservation were a pressure of 5 kPa and a temperature of 51ºC. Under these conditions, the corresponding responses of dried okra slices were 173 min for drying time, 0.24 %wb min^{-1} for drying rate, 1.44×10^{-9} m^2 s^{-1} for effective diffusivity, 32.6 kWh kg^{-1} for specific energy consumption, 12.64 for colour change, 0.75 for relative greenness, and 6.8 for rehydration ratio. Additionally, the findings demonstrated that the combination of pressures lower than 20 kPa with infrared drying effectively enhanced the performance factors of the dryer while preserving the colour of dried okra slices.

Keywords: Okra, Optimisation, Vacuum-infrared drying

Introduction

Okra (*Abelmoschus esculentus* L.), a warm-season crop, is predominantly cultivated for its immature pods in well-drained soils (Moosavi, Aghaalikhani, Ghobadian, & Fayyazi, 2018). In 2022, global okra production reached approximately 11.2 million tons, with 67.6% produced in Asia and 31.6% in Africa. Among the leading producers, India accounted for 61.2% of global production, followed by Nigeria (17%), Mali (6.8%), Pakistan (2.7%), and Sudan (2.6%) (FAO, 2020). Rich in fibre, vitamins, minerals, antioxidants, and high-quality protein, okra contributes to human health by supporting digestive health, lowering cholesterol, regulating blood sugar, and exhibiting antioxidant properties that may prevent chronic diseases. Okra also has diverse applications in food, industry, and medicine, functioning as a thickener, emulsifier, and pharmaceutical binder (Gemede, Ratta, Haki, Woldegiorgis, & Beyene, 2015). However, like most vegetables, okra is highly perishable because of its high moisture content, and the availability of fresh pods is limited to a short time frame. Traditionally, drying has been employed as a preservation method to extend the shelf life. Ismail, Kipcak, and Doymaz (2019) emphasised the need for efficient drying methods and reviewed the existing literature on various techniques for drying okra, highlighting limited research on infrared and vacuum drying methods. Vacuum-infrared drying is an efficient method for preserving fruits and vegetables, combining the advantages of infrared radiation and vacuum drying (Nimmol, 2010). This technique offers higher energy efficiency, shorter drying times, and improved product quality compared to traditional methods (Zang *et al.*, 2024). The process involves exposing products to infrared radiation in a reduced-pressure chamber, which allows for lower drying temperatures and better preservation of nutritional content. Salehi (2020) provided an extensive review of the applications and potential of infrared (IR) drying systems for agricultural products, including fruits, vegetables, and grains. This study highlighted vacuum-infrared drying as a promising method that combined the advantages of IR radiation and vacuum pressure to enhance drying efficiency and product quality. Research has demonstrated that this method significantly reduces drying time and energy consumption for fruits such as grapefruit, lemon, and banana while preserving colour and texture. For vegetables such as mushrooms and pumpkin, vacuum-infrared drying improved moisture diffusivity, retained nutritional components, and minimised shrinkage. This method was identified as a sustainable approach for producing high-quality dried agricultural products with reduced energy costs. Recent studies have further explored okra drying methods. El-Mesery, Qenawy, Hu, and Alshaer (2023) investigated the drying characteristics and quality of okra pods using an infrared dryer. Their findings indicated that drying occurred during the falling rate period, with shorter drying times observed at higher radiation intensities and lower air velocities.

Innu, Somfan, Vivek, Pongpimol, and Sa-adchom (2024) examined the effects of infrared radiation-assisted vacuum drying on the moisture content, energy consumption, and colour properties of okra powder. Drying was conducted at a fixed pressure (7 kPa) and temperatures of 70, 80, and 90°C until the moisture content fell below 10% (wet basis). Higher temperatures reduced moisture content more quickly and consumed less energy than drying at 70°C. However, drying at 70°C produced okra powder with superior colour quality and was characterised by higher lightness and greenness. These results identified 70°C as the optimal drying temperature for preserving the quality of okra powder under vacuum conditions.

Despite these advancements, the combined vacuum–infrared drying technique for okra slices remains underexplored. This study aimed to address this gap by using a vacuum-infrared dryer designed and constructed to do the experiments. The primary objective of this study was to model and evaluate the effects of temperature and pressure on the drying process of okra slices. Response Surface Methodology was employed to design experiments and optimise drying conditions. In addition, we assessed the influence of input parameters on the qualitative properties of dried okra slices.

Materials and Methods

In this study, fresh okra pods with an initial moisture content of about 88% (wb) were supplied from the local market and stored at 4°C in a refrigerator. Okra pods of similar size were manually selected and washed with distilled water. The tapered heads and ends of the okra pods were then trimmed to a uniform shape. The 5-mm-thick pod slices were dried in the vacuum-infrared dryer designed and fabricated for the experiments (Fig. 1). Before the experiments, the physical properties (size, shape, density, moisture content, and colour) of the okra samples were determined. For each experiment, a calliper with an accuracy of 0.05 mm was used to determine the main dimensions of 30 okra pods. Then, as a shape index, the sphericity of each okra pod was determined using Eq. (1), where φ is the sphericity (%), and L, W, and T are the length (mm), width (mm), and thickness (mm) of the okra pods, respectively:

$$\varphi = \frac{(LWT)^{\frac{1}{3}}}{L} \times 100 \qquad (1)$$

True density of five randomly chosen pods was determined using the platform scale method (Eq. (2)). In Eq. (2), ρ_s is the sample true density (g cm^{-3}), and M_S, M_{dw}, and ρ_w are mass of the sample (g), mass of the displaced water (g), and distilled water density (g cm^{-3}), respectively:

$$\rho_s = \frac{M_S \times \rho_w}{M_{dw}} \qquad (2)$$

The initial moisture content of okra pods was determined by the oven method. Approximately 50 grams of the pod sample was finely ground and dried at 105ºC for 24 hours (Dadalı, Apar, & Özbek, 2007). To determine the colour of each sample of okra slices, its image was taken before and after drying using a light box and a camera. Then, each image was processed using ImageJ (V1.52) software to determine the Lab colour attributes. Processing included cropping, RGB to Lab conversion, segmentation, and measurement of colour characteristics of the samples. The *L* index is the brightness in the range of 0 (black) to 100 (white), and the *a* and *b* indices respectively measure the green (-) to red (+) and blue (-) to yellow (+) tones. The overall colour change of dried okra slices (ΔE) was calculated by Eq. (3), where L_0, a_0, and b_0 are the colour indices of the fresh okra slices before drying. Moreover, to estimate the green colour preservation of the dried sample, the greenness of the okra slices before and after drying was compared (Eq. (4)):

$$\Delta E = \sqrt{(L-L_0)^2+(a-a_0)^2+(b-b_0)^2} \tag{3}$$

$$Relative\ Greenness\ Index = \frac{a}{a_0} \tag{4}$$

The rehydration ratio (RR) curve of the dried samples was also determined in half-hour periods up to 270 min (Eq. (5)). In Eq. (5), W_D and W_R are the weights of the dry and rehydrated okra slices, respectively. For this experiment, the ratio of okra to water (1:30) was selected, and 5 gr of dried okra slices was soaked in 150 ml of water. At the end of each period, the okra slices were removed from the distilled water and the excess water was removed from the slices' surface using a dry tissue. Then they were weighed (Ismail *et al.*, 2019):

$$\mathrm{RR} = \frac{W_R}{W_D} \tag{5}$$

Moisture ratio curves and effective diffusivity

The moisture ratio (MR) represents the amount of water in the sample at a specific moment of the drying process compared to the total water contained in the sample. Therefore, the moisture ratio at any moment can be calculated based on the instantaneous moisture content and the initial moisture content of the sample. The moisture content at each moment can also be determined by using the initial moisture content of the sample at the beginning of the drying process and the weight loss at the desired moment. Therefore, to extract both *MC-t* and *MR-t* curves, the initial moisture content of the sample, the initial weight of the sample and the weight of the sample at any moment of the drying process are sufficient (Eq. (6)):

$$\mathrm{MR} = \frac{MC_t - MC_e}{MC_0 - MC_e} \tag{6}$$

where, *MR* is the moisture ratio, and MC_t, MC_0, and MC_e are the instantaneous moisture content at time *t*, initial moisture content, and equilibrium moisture content, respectively. Since MC_e cannot be determined during the drying process, the simplified Eq. (7) is usually used (El-Mesery *et al.*, 2023):

$$\mathrm{MR} = \frac{MC_t}{MC_0} \tag{7}$$

Based on the *MR-t* curves, the effective diffusivity (D_{eff}) was determined using Eq. (8). Here, *MR* represents the moisture ratio as a dimensionless parameter, and D_{eff} ($m^2\ s^{-1}$) denotes the effective moisture diffusivity. Additionally, *r* (m) and *t* represent the radius of the okra samples and drying time, respectively (Wang, Zhao, Wang, Hong, & Zhao, 2019):

$$\ln MR = \left[\frac{6}{\pi^2}\right] - \left[\frac{\pi^2 Defft}{r^2}\right] \tag{8}$$

Drying rate

The drying rate (DR) of each sample was calculated based on its total weight loss due to drying and the length of time that the weight loss occurred. The drying rate of okra slices was calculated according to Eq. (9), where MC_i and MC_f are the initial and final moisture content of the sample, and *dt* is the total drying time. All samples were dried up to 15% wb moisture content:

$$\mathrm{DR} = \frac{MC_i - MC_f}{dt} \tag{9}$$

Specific energy consumption

The energy consumed by the IR heater (Q_t) and the vacuum pump (Q_P) was measured using two separate meters. At the end of each experiment, the amount of lost water (M_W) was determined as the difference between the weight of the fresh wet sample and the weight of the dried sample and the specific energy consumption (SEC) was calculated using Eq. (10) (Ismail *et al.*, 2019):

$$\mathrm{SEC} = \frac{Q_t + Q_P}{M_W} \tag{10}$$

Vacuum-infrared dryer

The experimental setup (Fig.1), which included infrared heating lamps and a vacuum chamber, was capable of controlling the pressure and temperature and simultaneously monitoring the weight of the samples during the drying process. The infrared heater was equipped with three infrared lamps (NOOR Industries, Iran) that provided thermal energy up to a maximum power of 750 W. The distance between the lamps and the sample inside the chamber was 13 cm. A digital thermostat (Hanyoung nux-BR6, South Korea) was used to turn the lamps on and off to control the temperature. An online weighing system, consisting of a load cell (Zemic L6D, maximum load: 2.5 kg, China) along with a digital monitor (Tika, TD1000C, Iran), was used to monitor the weight of the okra samples during the drying process. The vacuum inside the chamber was maintained using a two-stage vacuum pump (Valeo, VE280N, China) and controlled by a pressure transmitter (Hogller, range: -1 to 1 bar, Germany) and a PID controller (Adonis TMC-N, Iran). The research process layout is shown in Fig. 2.

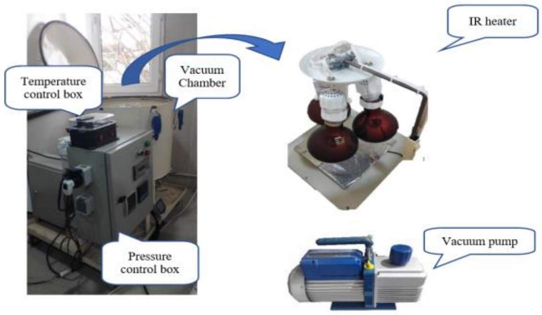

Fig. 1. The Vacuum-infrared dryer used for drying okra slices

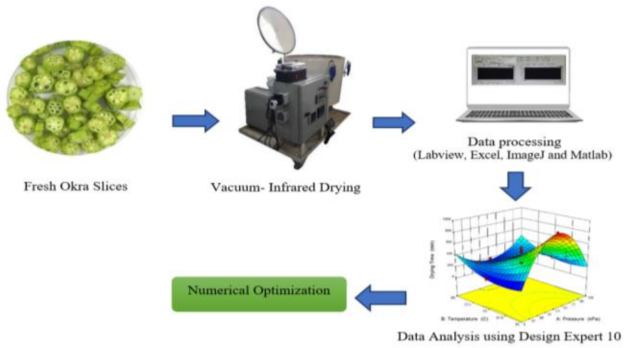

Fig. 2. Schematic diagram of the research process

Experimental data for the vacuum-infrared drying of okra slices were collected under various levels of the independent variables (pressure and temperature) and utilised for developing the response surface methodology (RSM). RSM was used to determine the relationship between input and response variables (Elena Vivanco-Cuba & Vivanco-Pezantes, 2025). In this study, a five-level central composite design was employed for the examined factors (Ardebili, Babagiray, Aytav, Can, & Boroiu, 2022). The designed CCD-based RSM matrix is presented in Table 1.

Table 1- Coded levels of the drying process independent variables

Independent variable	X_i	coded levels				
		-α	-1	0	+1	+α
A: Pressure (kPa)	X_1	5	21	53	85	101
B: Temperature (ºC)	X_2	50	55	65	75	80

Results and Discussion

Physical properties of the okra samples

The physical properties of the fresh okra pods are represented in Table 2.

The summarised ANOVA results are presented in Tables 3 and 4. The quadratic model was the best predictive model for both quantitative and qualitative parameters, except for DT, where the reduced cubic model performed the best. The lack of fit was non-significant for all the parameter analyses.

Table 2- Physical properties of the okra pods

Physical property	Average	Standard deviation	Confidence interval (95%)
Length (mm)	42.9	9.2	42.9±0.6
Width (mm)	13.8	2.2	13.8±0.1
Thickness (mm)	12.6	1.6	12.6±0.1
Sphericity (%)	46.2	5.2	46.2±0.3
Density (gr cm^{-3})	0.77	0.07	0.77±0.01
Mass (g)	3.2	0.9	3.2±0.9
L	50.7	3.5	50.7±1.3
a	-15.8	0.9	-15.8±0.3
b	40	2.4	40±0.9

Table 3- ANOVA results for the quantitative properties of the drying process of okra slices

	DT		DR		D_{eff}		SEC	
Source	df	F-Value	df	F-Value	df	F-Value	df	F-Value
Model	6	63.66 **	5	34.95 **	5	58.22 **	5	7.24 **
A-Pressure	1	0.98 ns	1	1.85 ns	1	1.24 ns	1	0.22 ns
B-Temperature	1	250.02 **	1	28.14 **	1	169.27 **	1	15.81 **
AB	1	2.968E-03 ns	1	0.093 ns	1	1.18 ns	1	0.091 ns
A^2	1	49.71 **	1	64.21 **	1	69.03 **	1	14.16 **
B^2	1	17.32 **	1	3.62 ns			1	17.41 **
A^2B	1	46.60 **			1	14.14 **		
Residual	21		20		23		22	
Lack of Fit	2	0.40 ns	2	2.32 ns	3	1.95 ns	3	1.23 ns
Pure Error	19		18		20		19	
Cor Total	27		25		28		27	

** significant at 99% level of confidence, *ns* not significant

Table 4- ANOVA results for the qualitative properties of the dried okra slices

		ΔE	a/a_0	RR_{180min}
Source	df	F-Value	F-Value	F-Value
Model	5	5.98 **	19.37**	5.11**
A-Pressure	1	4.37 *	28.15**	2.61 ns
B-Temperature	1	7.75 **	28.49**	12.26**
AB	1	0.046 ns	1.44 ns	0.93 ns
A^2	1	12.13 **	34.91**	1.54 ns
B^2	1	0.040 ns	2.01 ns	3.22 ns
Residual	23			
Lack of Fit	3	1.24 ns	1.30 ns	0.42 ns
Pure Error	20			
Cor Total	28			

** significant at 99% level of confidence, ns not significant

Drying time

The results of the vacuum-infrared drying of okra slices demonstrated a significant impact of the drying conditions on the drying time at a 1% statistical significance level, indicating that the reduced cubic model could effectively predict the experimental data. As indicated in Table 3, pressure (A^2 and A^2B) and temperature (B and B^2) had statistically significant effects on drying time at the 1% level. The following reduced cubic equation (Eq. (11)), based on pressure and temperature, was derived using the response surface methodology (RSM) models:

$$\begin{aligned} \mathbf{DT}\ (\mathbf{min}) = &+410.86 \\ &+ (10.39 \times A) \\ &- (253.65 \times B) \\ &+ (0.83 \times AB) \\ &- (98.22 \times A^2) \\ &+ (60.21 \times B^2) \\ &+ (151.31 \times A^2B) \end{aligned} \qquad (11)$$

According to the results depicted in Fig. 3, the longest drying time (927 min) occurred at the point corresponding to the minimum temperature (50°C) and an intermediate pressure (53.4 kPa) within the range of pressure variations. As expected, an increase in temperature from 50 to 80°C reduced the drying time of the samples. However, the effect of pressure had a different trend. Both increasing and decreasing the pressure from its intermediate value resulted in a gradual reduction in drying time. Consequently, the shortest drying times were observed at the minimum and maximum pressure levels (5 and 101 kPa). This trend is further confirmed by the significance of the quadratic pressure effect in the analysis of variance. Ismail *et al.* (2019) compared the drying time of okra using five drying methods. Microwave drying was the fastest method, requiring only 46 minutes, while sun drying was the slowest, requiring 50 hours. For the other three methods of hot-air drying (50°C), vacuum oven drying (50°C), and infrared drying, the drying times were 13.5 hours, 10 hours, and 9.25 hours, respectively (Ismail *et al.*, 2019). Previously, Afolabi and Agarry (2014) reported drying times of 10 to 13 hours for hot-air drying at temperatures ranging from 50 to 70°C.

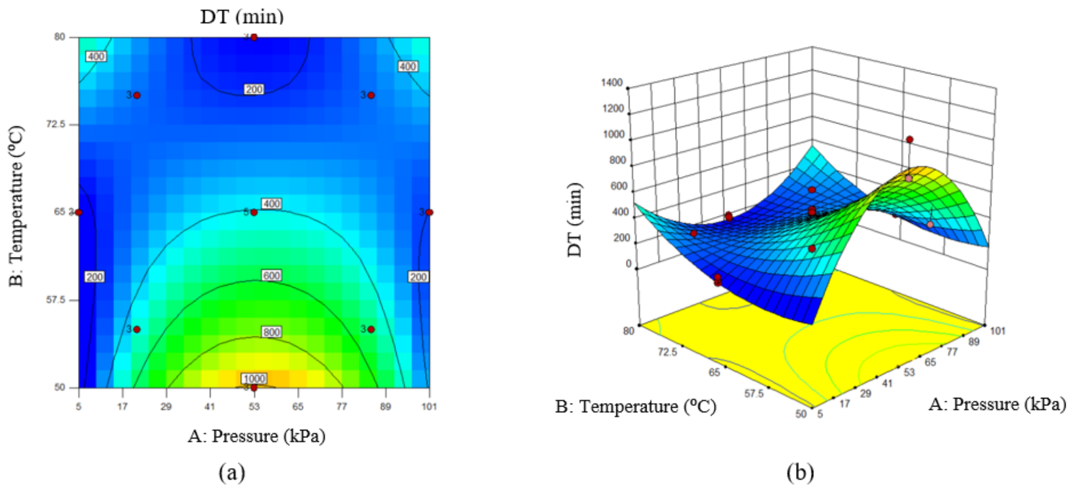

Fig. 3. (a) 2D and (b) 3D plots of the combined effect of temperature and pressure on the drying time of okra slices

Drying rate

The effects of pressure (A^2) and temperature (B) on the drying rate of okra slices were statistically significant at the 1% level (Table 3). The F-value and P-value results in Table 3 indicate that pressure had the most significant effect on the drying rate of okra, with an F-value of 64.21. Temperature exhibits a great impact on the drying rate as well, as evidenced by an F-value of 28.14. The derived formula for the quadratic model is given in Eq. (12):

$$\mathbf{DR}\ (\%\mathbf{wb\ min^{-1}}) = +0.17 - (0.01 \times A) + (0.053 \times B) - (3.33 \times 10^{-3} \times AB) + (0.08 \times A^2) - (0.023 \times B^2) \quad (12)$$

As shown in Figure 4a, the minimum drying rate (0.06 %wb min^{-1}) occurred around the point corresponding to the intermediate pressure and minimum temperature (blue-shaded area). A gradual increase or decrease in pressure from this point led to an increase in the drying rate. Therefore, to achieve higher drying rates for the samples, pressures near the minimum (5 kPa) or maximum (101 kPa) are recommended. However, it should be noted that among these, pressures near 5 kPa have a more pronounced effect, as highlighted by the red area in the figure. Additionally, the drying rate was directly related to the drying time. As shown in Figure 4b, increasing the temperature from 50 to 80°C resulted in a sharp rise in the drying rate. The maximum drying rate predicted by the model is 0.41 (%wb min^{-1}), occurring at (5 kPa, 77.5°C).

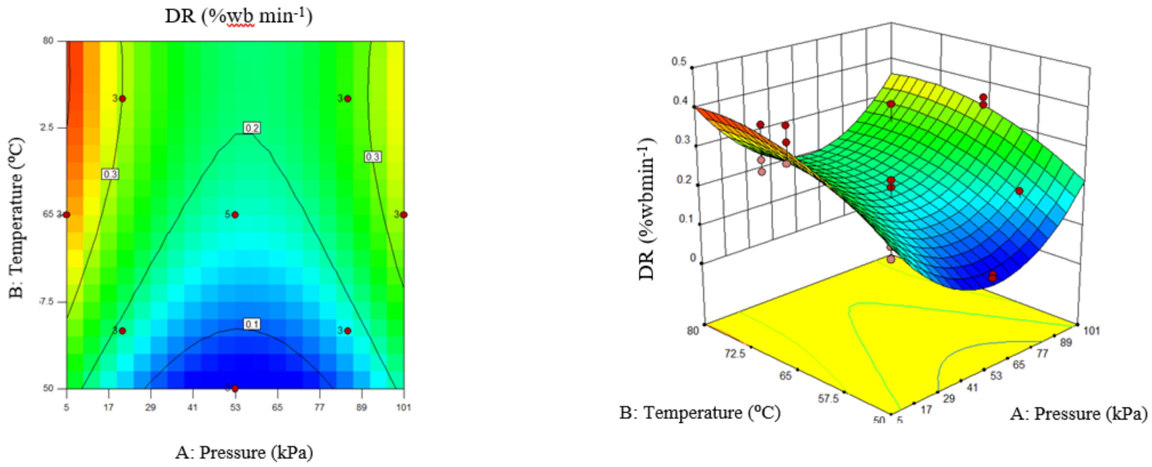

(a) (b)

Fig. 4. (a) 2D and (b) 3D plots of the interaction impact of temperature and pressure on the drying rate of okra slices

Effective Diffusivity

Based on the analysis of variance (ANOVA) presented in Table 3, pressure (A^2, A^2B) and temperature (B) have a significant impact on D_{eff} at the 1% significance level. The corresponding model is presented in Eq. (13):

$$\mathbf{log(Deff)} = -9.20 - (0.016 \times A) + (0.25 \times B) + (0.022 \times AB) + (0.13 \times A^2) - (0.11 \times A^2B) \quad (13)$$

The smallest amount of D_{eff} (2.68×10^{-10}) occurs in the lowest drying temperature (50°C) and pressures around the intermediate pressure (55.7 kPa) (Fig. 5). As the temperature increases, D_{eff} also increases. Applying pressures near 5 kPa or 101 kPa increased the effective diffusivity. The maximum D_{eff} (i.e. 1.43×10^{-9}) can be achieved either in (5 kPa, 50°C) or (101 kPa, 80°C). Selecting a pressure near 5 kPa is more advisable from the perspective of preserving product quality because it allows the use of lower temperatures without significantly reducing the effective diffusion coefficient. Tanta and Doymaz (2019) observed that increasing infrared dryer power from 62 to 104 W resulted in an increase in the effective diffusion coefficient from 8.54×10^{-10} to 2.32×10^{-9} m² s^{-1}. Similarly, El-Mesery *et al.* (2023) investigated infrared drying of okra and reported effective diffusivity values ranging from 2.89×10^{-10} to 12.23×10^{-10} m² s^{-1}, which fall within the typical range for food materials. Ghaboos, Ardabili, Kashaninejad, Asadi, and

Aalami (2016) examined vacuum-infrared drying of pumpkin and found that effective diffusivity increased with infrared power, ranging from 0.71×10^{-9} to 2.86×10^{-9} m² s^{-1}. Li *et al.* (2019) reported effective diffusivity values for hot-air drying ranging from 0.992×10^{-9} to 4.409×10^{-9} m² s^{-1}, and from 1.915×10^{-9} to 5.291×10^{-9} m² s^{-1} for heat pump drying.

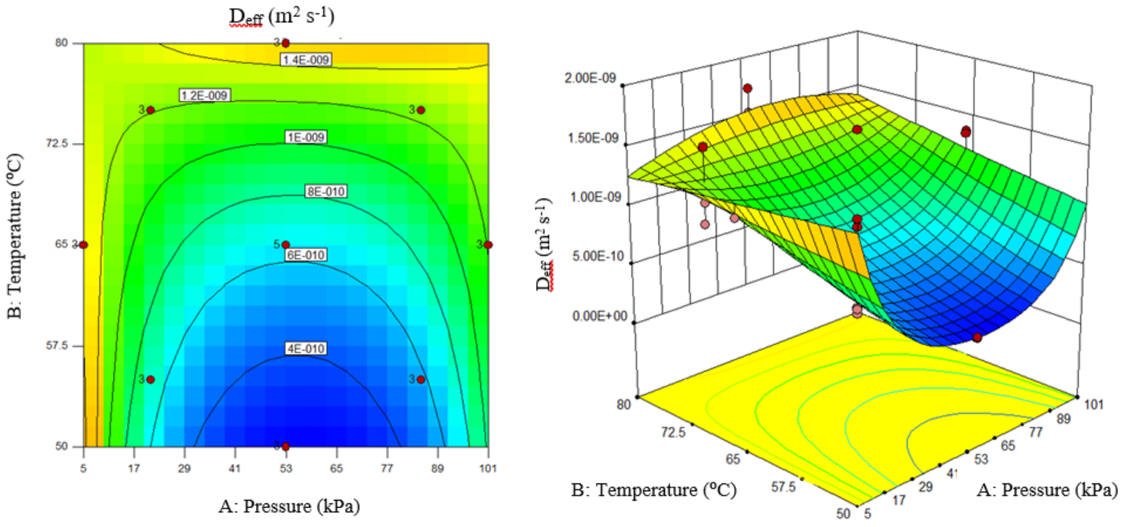

(a) (b)

Fig. 5. (a) 2D and (b) 3D plots of the interaction effect of temperature and pressure on D_{eff} of okra slices

Specific energy consumption (SEC)

As shown in Table 3, the effects of pressure (A^2) and temperature (B, B^2) on specific energy consumption were significant at 1% level. The derived formula for the quadratic model is given in Eq. (14).

$$\textbf{SEC}\ (\text{kWh}\ kg^{-1}) = +51.91 + (0.51\times A) - (4.29\times B) + (0.48\times AB) - (5.78\times A^2) - (6.41\times B^2) \quad (14)$$

Given the significance of the model, it can be concluded that the derived model effectively predicts the experimental SEC data. Figure 6 illustrates the 2D and 3D diagrams, showing the effect of the input variables on SEC.

As illustrated in Figure 6a, the central region (54 kPa and 61.7°C) exhibits the highest specific energy consumption (52.6 kWh kg^{-1}), while the lowest value for this parameter (20.9 kWh kg^{-1}) occurs at atmospheric pressure and 80°C. At atmospheric pressure, the vacuum pump is shut down, resulting in lower energy consumption. Interestingly, the use of a vacuum pump to achieve a pressure of 5 kPa at both low temperatures (lower left corner) and high temperatures (upper left corner) is also favourable in terms of the overall specific energy consumption. Innu *et al.* (2024) demonstrated that vacuum-infrared drying of okra sheets at 7 kPa and 70°C resulted in significantly higher electrical energy and specific energy consumption than drying at 80 and 90°C.

Kumar, Prasad, and Murthy (2014) reported the specific energy consumption for drying okra using method A (temperatures between 40-70°C and air velocities ranging 1-2 m s^{-1}) to be in the range of 40.52 to 96.6 MJ kg^{-1}, equivalent to 11.26-26.83 kWh kg^{-1}. Ismail *et al.* (2019) reported the specific energy consumption of drying okra using different methods as follows: vacuum oven drying (69.95 kWh kg^{-1}), hot-air drying (27.4 kWh kg^{-1}), infrared drying (22.82 kWh kg^{-1}), and microwave drying (20.54 kWh kg^{-1}).

A:

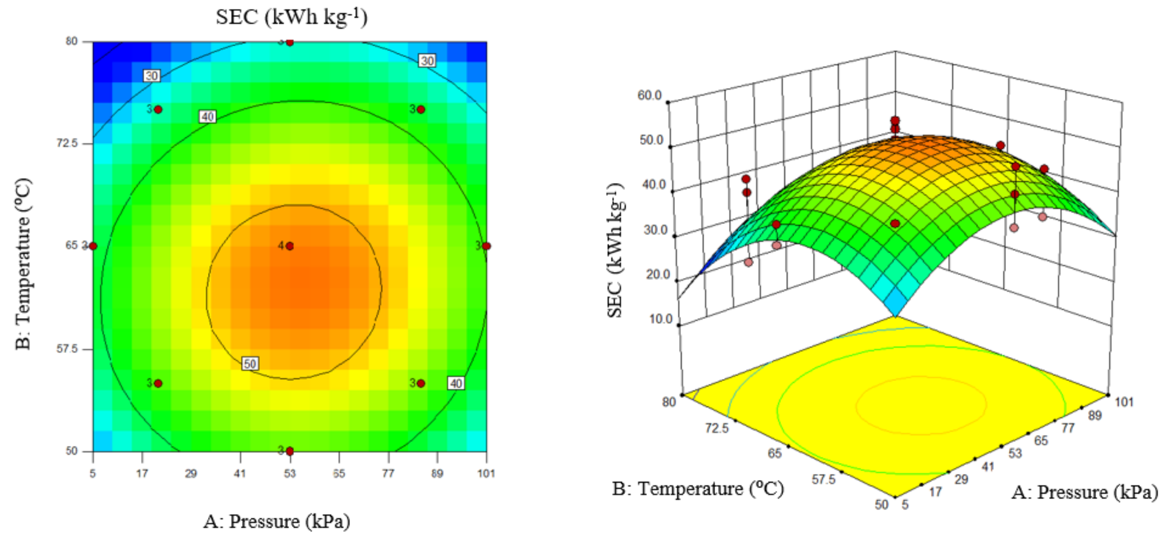

(a) (b)

Fig. 6. (a) 2D and (b) 3D plots of the interaction effect of temperature and pressure on the SEC of okra slices

Colour change

ANOVA results (Table 4) demonstrate that the effect of pressure (A^2) and temperature (B) on the overall colour change (ΔE) of okra slices is statistically significant at the 1% level. The derived formula for ΔE is given in Eq. (15):

$$\Delta \mathbf{E} = +24.51 + (1.41 \times A) + (1.88 \times B) - (0.21 \times AB) - (3.12 \times A^2) + (0.18 \times B^2) \quad (15)$$

As the drying temperature increases, there is a more pronounced change in the overall colour of the dried okra slices (Fig. 7). The minimal colour change (ΔE = 12.47) was obtained by concurrently applying 50 °C and 5 kPa. By applying a pressure of 5 kPa, it can be ensured that even by increasing the dryer temperature to 62.7 °C, the ΔE value will not exceed 15.

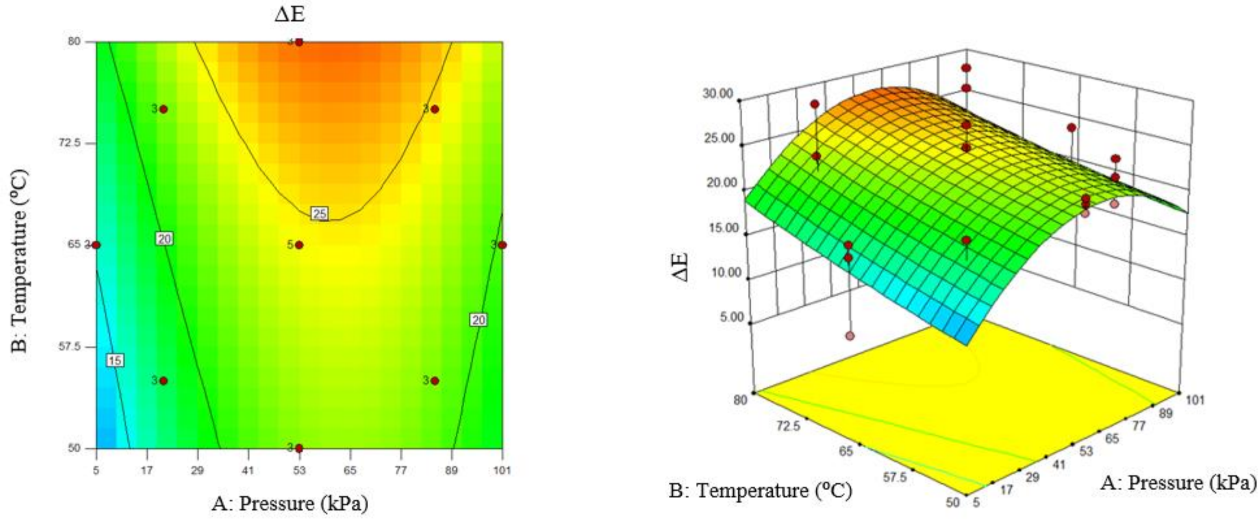

(a) (b)

Fig. 7. (a) 2D and (b) 3D plots of the interaction impact of temperature and pressure on the ΔE of okra slices

Ismail *et al.* (2019) examined the overall colour change in fresh okra, characterised by average *L*, *a*, and *b* values of 42.69, -3.6, and 8.34, respectively, following drying using five different methods: vacuum oven drying (50°C, 0.1 kPa), sunlight drying, microwave drying, infrared drying, and hot air drying (50°C). The reported overall colour change (ΔE) values were 10.64, 18.93, 13.54, 11.15, and 9.62, respectively. Innu *et al.* (2024) reported that okra powder dried at higher temperatures showed significantly reduced lightness (L value) and greenness (-a value) compared to those dried at lower temperatures. As a result, drying okra powder at an absolute chamber pressure of 7 kPa and a temperature of 70°C yielded superior colour quality compared to samples dried at 80°C and 90°C.

Relative Greenness Index

The relative greenness index (a/a_0) of dried okra slices was significantly influenced by both pressure (A, A^2) and drying temperature (B) (Table 4). Eq. (16) gives the derived formula for a/a_0:

$$\frac{a}{a_0} = +0.21 - (0.086 \times A) - (0.086 \times B) - (0.028 \times AB) + (0.13 \times A^2) + (0.03 \times B^2) \quad (16)$$

According to Fig. 8, as the drying temperature increased, the relative green colour (a/a_0) substantially decreased. Conversely, lower pressure is associated with improved retention of the green colour. Optimal conditions for maintaining the green colour of okra slices ($a/a_0 > 0.7$) were achieved at pressures below 10 kPa and temperatures below 55°C. The best conditions for preserving the green colour of the samples were 5.4 kPa and 50°C, whereas the worst conditions were 69.2 kPa and 80°C. The index for these two points was determined to be 0.75 and 0.12, respectively. According to Ismail *et al.* (2019), the *a* values for the dried samples were 6.8 (vacuum oven), 11.38 (sunlight), 4.85 (microwave), 5.39 (infrared), and 3.67 (hot air). The transition of the *a* values from negative in fresh okra to positive in all dried samples indicates a shift in the predominant green hue of fresh okra toward a red hue across all drying methods.

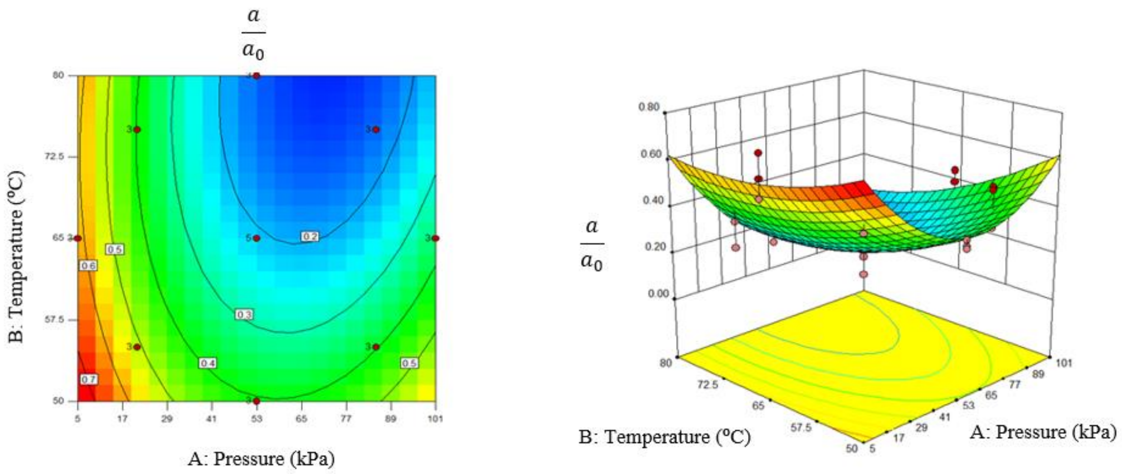

(a) (b)

Fig. 8. (a) 2D and (b) 3D plots of the interaction impact of temperature and pressure on the a/a_0 of okra slices

The effect of high temperature and high pressure on the green colour degradation in the dried samples is visible in Figure 9. The images on the left depict fresh samples, while those on the right show the same samples after drying. As observed, the use of lower temperatures combined with reduced pressure has effectively preserved the green colour.

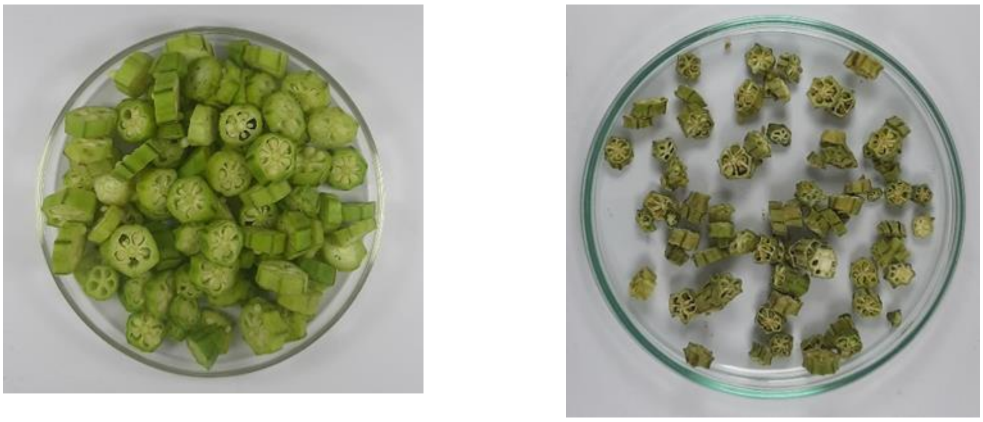

P = 5 kPa and T = 65 ºC

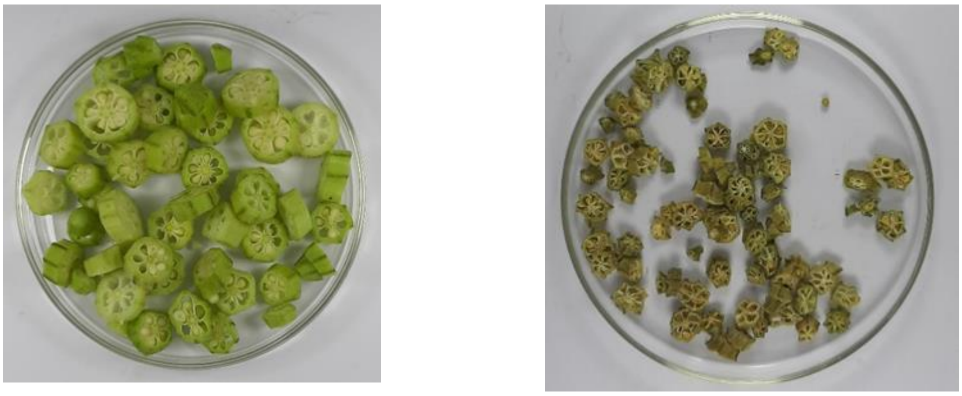

P = 85 kPa and T = 75 ºC

Fig. 9. The impact of temperature and pressure on the green colour preservation of okra slices

Rehydration ratio (RR)

As shown in Table 4, the effect of pressure on RR was not statistically significant. However, temperature significantly affected the RR. Eq. (17) gives the derived formula for RR:

$$\mathbf{RR}\ (180\text{min}) = +7.61 - (0.19 \times \text{A}) + (0.42 \times \text{B}) - (0.17 \times \text{AB}) + (0.2 \times \text{A}^2) - (0.29 \times \text{B}^2) \quad (17)$$

As illustrated in Fig.10, RR exhibits an increasing trend with increasing temperature from 50 to 80°C. Specifically, based on the model's predicted data, the maximum RR value (i.e., 8.8) was achieved at a temperature of 76.4°C and a pressure of 5 kPa, while the minimum value (i.e., 6.3) was obtained at a temperature of 50°C and a pressure of 48.3 kPa. Fig. 11 shows the RR variation curve over the 270-min period. In Figure 11a, the effect of drying temperature at a constant pressure of 53 kPa is clearly visible. In Figure 11b, the impact of dryer pressure on the RR of the dried samples was somewhat observable. Although the curves are very close to each other (indicating a non-significant pressure effect), the curve for a pressure of 5 kPa is slightly higher than the other two curves.

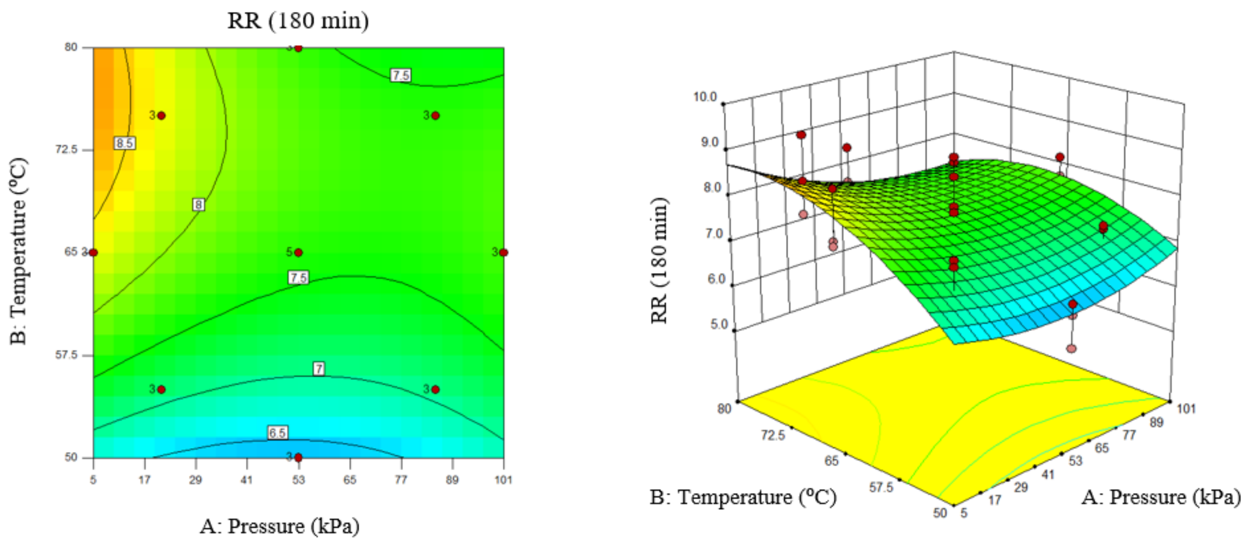

(a) (b)

Fig. 10. (a) 2D and (b) 3D plots of the interaction impact of temperature and pressure on the RR (180min) of okra slices

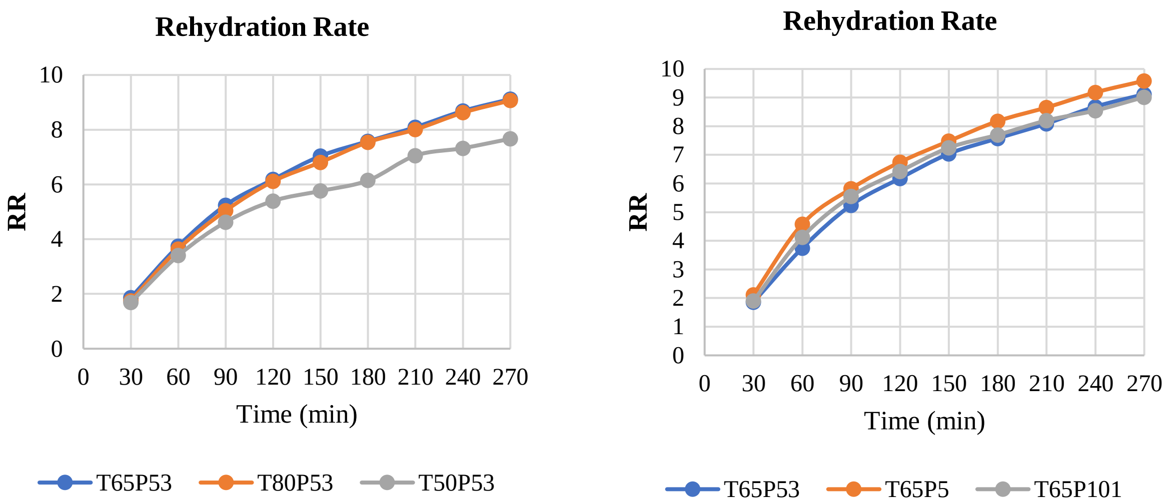

(a) (b)

Fig. 11. RR change of okra slices over time at fixed (a) P = 53 kPa, and (b) T = 65 °C

Ismail *et al.* (2019) reported the rehydration ratio of dried okra samples processed using hot air, sunlight, infrared, vacuum oven, and microwave drying methods to be 4.86, 4.39, 4.25, 4.12, and 3.35 (g $_{water}$ / g $_{dry\ matter}$), respectively. In other words, the RR ranged from 4.35 to 5.86 g (g $_{rehydrated\ sample}$ / g $_{dry\ sample}$). Furthermore, El-Mesery *et al.* (2023) determined the rehydration ratio of okra pods dried using microwave, infrared, and hot air methods to range from 3.35 to 4.49 (g $_{wet\ sample}$ / g $_{dry\ sample}$).

Optimisation

The optimisation of vacuum-infrared drying of okra slices was conducted considering various scenarios including: (A) minimising drying time, (B) maximising the preservation of the green colour in the dried samples, (C) minimising drying time while maintaining the green colour of the dried samples, and (D) simultaneously minimising drying time and ΔE while maximising the green colour and rehydration ratio. The measured parameters and the optimal operating conditions of the dryer for each scenario are presented in Table 5. Fig. 12 illustrates the optimal regions for dryer operating conditions in each scenario. As observed, regions near a pressure of 5 kPa exhibit high desirability across all scenarios. In contrast, regions near a pressure of 101 kPa (drying at atmospheric pressure) may be justifiable in terms of drying time and specific energy consumption but are less favourable for preserving product quality.

Table 5- Recommended settings (P, T) and the corresponding predicted results for drying okra slices

Scenario	*P* *kPa*	*T* *°C*	Parameter						
			DT	DR	D_{eff}	SEC	ΔE	a/a_0	RR
A	*5.8*	*58*	159.2	0.31	1.35E-09	38.9	14.18	0.66	7.7
B	*5.8*	*50*	205.9	0.23	1.37E-09	31.6	12.75	0.75	6.7
C	*5*	*51*	172.6	0.24	1.44E-09	32.6	12.67	0.75	6.8
D	*5*	*63*	161	0.36	1.36E-09	38.8	14.98	0.63	8.2

The selection of the desired scenario depends on the user's perspective. It appears that colour attributes, due to their immediate impact on the consumer's perception of the final product, hold greater importance than other characteristics. Therefore, if scenario C was selected, the optimal adjustment of the drying process would be (5 kPa, 51°C). Under these conditions, the drying time, drying rate, effective diffusivity (D_{eff}), specific energy consumption (SEC), ΔE, relative greenness (a/a_0), and rehydration ratio (RR) would be 173 min, 0.24%wb min^{-1}, 1.44×10^{-9} m^2 s^{-1}, 32.6 kWh kg^{-1}, 12.64, 0.75, 6.8, respectively.

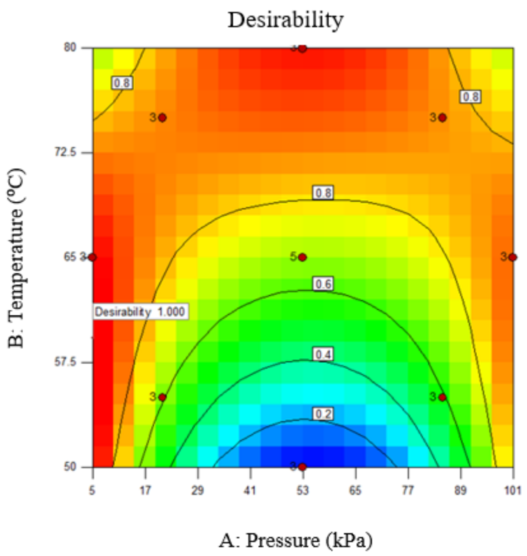

A: Minimising DT

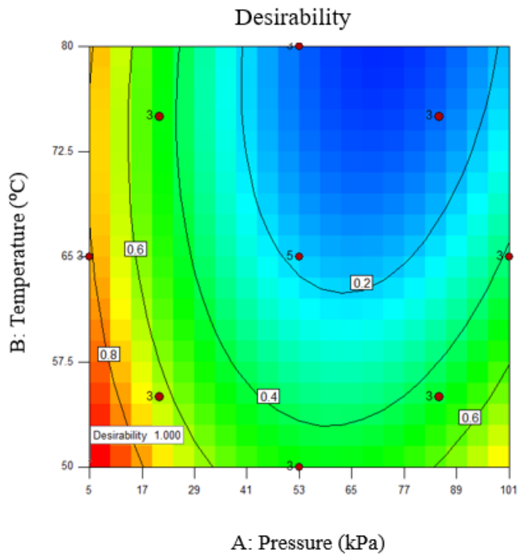

B: Maximising a/a_0

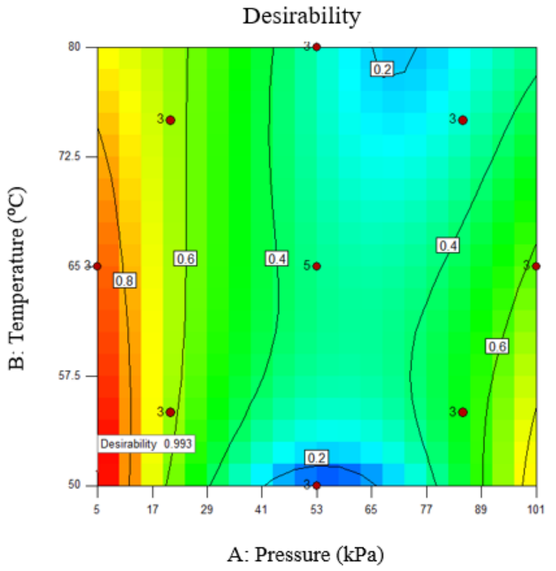

C: Minimising DT and Maximising a/a_0

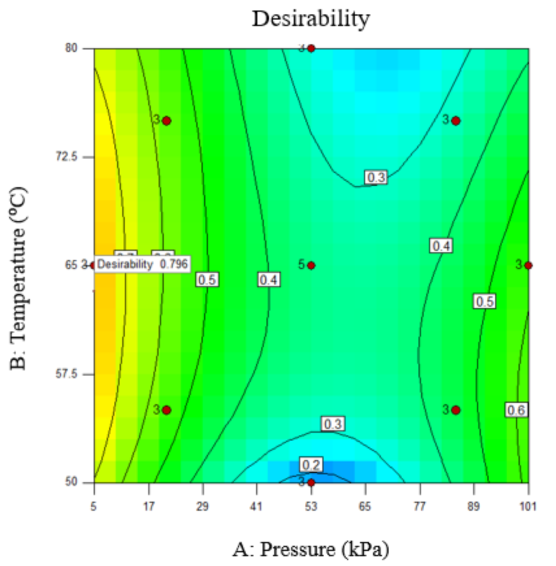

D: Minimising (DT, E) and Maximising (a/a_0, RR)

Fig. 12. 2D plot of the optimised drying conditions of okra slices for the four scenarios: A, B, C, and D

Conclusion

In this study, okra slices were dried using a vacuum-assisted infrared drying method. Five levels of temperature (50, 55, 65, 75, and 80°C) and pressures (5, 21, 53, 85, and 101 kPa) were considered as input parameters, and the output traits were drying time, drying rate, effective diffusivity, specific energy consumption, colour change, and rehydration ratio. The results indicated that temperature significantly affected all measured attributes. An increase in temperature improved certain attributes, such as drying time, drying rate, effective diffusion coefficient, specific energy consumption, and rehydration ratio. However, this also increased the overall colour change of the dried sample and resulted in a more pronounced loss of its green colour. Pressure also had a highly significant effect on most measured attributes, except for the rehydration ratio of the dried samples. Notably, in most of the variance analyses, the quadratic term of pressure was significant. This indicates that very low and very high pressures (the extremes of the pressure range studied) had more favourable effects than intermediate pressure levels. Therefore, if a reduced vacuum is to be used as an aid in the infrared drying process, very low pressures (e.g., below 20 kPa) should be employed. Using higher pressures offers no advantage over the use of infrared radiation alone (at atmospheric pressure) and is not justifiable. Considering the objective of minimising drying time while simultaneously preserving the green colour of the dried samples, the optimal drying process settings were determined to be (5 kPa, 51 °C). Under these conditions, the drying time, drying rate, effective diffusivity (D_{eff}), specific energy consumption (SEC), ΔE, relative greenness (a/a_0), and rehydration ratio (RR) were 173 min, 0.24%wbmin^{-1}, 1.44×10^{-9} m^{2}s^{-1}, 32.6 kWhkg^{-1}, 12.64, 0.75, and 6.8, respectively.

Compliance with Ethical Standards

Conflict of interest: The authors declare that they have no conflicts of interest.

Funding: This work was supported by Shahid Chamran University of Ahvaz [grant number SCU.AA1401.646].

Acknowledgements

The authors appreciate Shahid Chamran University of Ahvaz for the financial support of the project.

Author Contributions

F. SalehNezhad: Doing the experiments, Data acquisition and preparation, Visualization, and Preparing the manuscript

Y. Mansoori: Supervision, Conceptualization, Designing and fabrication of the laboratory- scale dryer, Methodology, Technical advice, Data processing and analysis, and preparing the manuscript

S. M. Safieddin Ardebili: Data post processing, Statistical analysis using Design Expert software, and preparing the manuscript

References

1. Afolabi, T. J., & Agarry, S. E. (2014). Thin layer drying kinetics and modelling of okra (*Abelmoschus esculentus* (L.) Moench) slices under natural and forced convective air drying. *Food Science and Quality Management*, *28*(6), 35-49. https://doi.org/10.1016/j.lwt.2019.05.099
2. Ardebili, S. M. S., Babagiray, M., Aytav, E., Can, Ö., & Boroiu, A.-A. (2022). Multi-objective optimization of DI diesel engine performance and emission parameters fueled with Jet-A1–Diesel blends. *Energy*, *242*, 122997. https://doi.org/10.1016/j.energy.2021.122997
3. Dadalı, G., Apar, D. K., & Özbek, B. (2007). Estimation of effective moisture diffusivity of okra for microwave drying. *Drying Technology*, *25*(9), 1445-1450.
4. El-Mesery, H. S., Qenawy, M., Hu, Z., & Alshaer, W. G. (2023). Evaluation of infrared drying for okra: Mathematical modelling, moisture diffusivity, energy activity and quality attributes. *Case Studies in Thermal Engineering*, *50*, 103451. https://doi.org/10.1016/j.csite.2023.103451
5. Elena Vivanco-Cuba, E., & Vivanco-Pezantes, D. (2025). Optimization of Hot-Air Drying Assisted with Incandescent Lamp of Red Seaweed (*Chondracanthus chamissoi*) Using Response Surface Methodology. *Journal of Agricultural Machinery*. https://doi.org/10.22067/jam.2025.89911.1283
6. FAO. (2020). FAO, 2020. www.fao.org. Retrieved from https://www.fao.org/faostat/en/#data/QCL
7. Gemede, H. F., Ratta, N., Haki, G. D., Woldegiorgis, A. Z., & Beyene, F. (2015). Nutritional quality and health benefits of okra (*Abelmoschus esculentus*): A review. *Journal of Food Processing & Technology*, *6*(458), 2.
8. Ghaboos, S. H. H., Ardabili, S. M. S., Kashaninejad, M., Asadi, G., & Aalami, M. (2016). Combined infrared-vacuum drying of pumpkin slices. *Journal of Food Science and Technology*, *53*(5), 2380-2388. https://doi.org/10.1007/s13197-016-2212-1
9. Innu, P., Somfan, N., Vivek, S., Pongpimol, S., & Sa-adchom, P. (2024). Effect of drying temperature level on vacuum drying of okra combined with far-infrared radiation. *RMUTP Research Journal Sciences and Technology*, *18*(1), 67-78.
10. Ismail, O., Kipcak, A. S., & Doymaz, I. (2019). Drying of okra by different drying methods: Comparison of drying time, product color quality, energy consumption and rehydration. *Athens Journal of Sciences*, *6*, 155-168.
11. Kumar, D., Prasad, S., & Murthy, G. S. (2014). Optimization of microwave-assisted hot air drying conditions of okra using response surface methodology. *Journal of Food Science and Technology*, *51*(2), 221-232. https://doi.org/10.1007/s13197-011-0487-9
12. Li, H., Xie, L., Ma, Y., Zhang, M., Zhao, Y., & Zhao, X. (2019). Effects of drying methods on drying characteristics, physicochemical properties and antioxidant capacity of okra. *Lwt*, *101*, 630-638. https://doi.org/10.1016/j.lwt.2018.11.076
13. Moosavi, S. A., Aghaalikhani, M., Ghobadian, B., & Fayyazi, E. (2018). Okra: A potential future bioenergy crop in Iran. *Renewable and Sustainable Energy Reviews*, *93*, 517-524. https://doi.org/10.1016/j.rser.2018.04.057
14. Nimmol, C. (2010). Vacuum far-infrared drying of foods and agricultural materials. *The Journal of the King Mongkut's University of Technology North Bangkok*, *20*, 37-44.

15. Salehi, F. (2020). Recent applications and potential of infrared dryer systems for drying various agricultural products: A review. *International Journal of Fruit Science*, *20*(3), 586-602. https://doi.org/10.1080/15538362.2019.1616243
16. Tanta, S., & Doymaz, İ. (2019). Drying of okra by infrared radiation. *Sigma Journal of Engineering and Natural Sciences*, *37*(1), 93-104.
17. Wang, H., Zhao, Q.-S., Wang, X.-D., Hong, Z., & Zhao, B. (2019). Pretreatment of ultrasound combined vacuum enhances the convective drying efficiency and physicochemical properties of okra (*Abelmoschus esculentus*). *Lwt*, *112*, 108201. https://doi.org/10.1016/j.lwt.2019.05.099
18. Zang, Z., Wan, F., Ma, G., Xu, Y., Wang, T., Wu, B., & Huang, X. (2024). Enhancing peach slices radio frequency vacuum drying by combining ultrasound and ultra-high pressure as pretreatments: Effect on drying characteristics, physicochemical quality, texture and sensory evaluation. *Ultrasonics Sonochemistry*, *103*, 106786. https://doi.org/10.1016/j.ultsonch.2024.106786

خشک‌کردن خلأ- مادون‌قرمز برش‌های بامیه: بررسی سینتیک، تحلیل کیفیت و بهینه‌سازی چندمنظوره

فاطمه صالح نژاد[1]، یعقوب منصوری[1*]، صفی الدین اردبیلی[1]

تاریخ دریافت: ۱۴۰۴/۰۴/۰۸
تاریخ پذیرش: ۱۴۰۴/۰۹/۳۰

چکیده

برش‌های گیاه بامیه (*Abelmoschus esculentus* L.) با استفاده از روش خشک‌کردن خلأ- مادون‌قرمز خشک شدند. یک خشک‌کن آزمایشگاهی در مقیاس کوچک طراحی و ساخته شد تا امکان کنترل پارامترهای خشک‌کردن و پایش تغییرات وزنی نمونه‌ها فراهم گردد. پارامترهای مورد بررسی شامل دما (در بازه ۵۰ تا ۸۰ درجه سلسیوس) و فشار (در محدوده ۵ تا ۱۰۱ کیلوپاسکال) بودند. عوامل پاسخ شامل زمان خشک‌کردن، سرعت خشک‌کردن، ضریب نفوذ مؤثر، مصرف ویژه انرژی، تغییر رنگ، سبزفامی نسبی و نسبت بازجذب آب بودند. نتایج حاصل از روش سطح پاسخ نشان داد که شرایط بهینه برای حداقل‌سازی زمان خشک‌کردن و حداکثرسازی حفظ رنگ سبز، فشار ۵ کیلوپاسکال و دمای ۵۱ درجه سلسیوس است. در این شرایط، مقادیر حاصل برای زمان خشک شدن ۱۷۳ دقیقه، سرعت خشک شدن ۰/۲۴ درصد رطوبت (بر مبنای تر) بر دقیقه، ضریب انتشار مؤثر $۱/۴۴ \times ۱۰^{-۹}$ متر مربع بر ثانیه، انرژی مصرفی ویژه ۳۲/۶ کیلووات ساعت بر کیلوگرم، تغییر رنگ ۱۲/۶۴، سبزفامی نسبی ۰/۷۵ و نسبت بازجذب آب ۶/۸ بودند. علاوه بر این، یافته‌ها نشان دادند که ترکیب فشارهای کمتر از ۲۰ کیلوپاسکال با خشک‌کردن مادون‌قرمز به‌طور مؤثری موجب بهبود شاخص‌های عملکرد خشک‌کن شده و در عین حال رنگ برش‌های خشک‌شده بامیه را حفظ می‌نماید.

واژه‌های کلیدی: بامیه، بهینه‌سازی، خشک کردن در خلاء-مادون قرمز

۱- گروه مهندسی بیوسیستم، دانشکده کشاورزی، دانشگاه شهید چمران اهواز، اهواز، ایران
(*- نویسنده مسئول: Email: y.mansoori@scu.ac.ir)

https://doi.org/10.22067/jam.2025.96137.1442